Application of slip-band visualization technique to tensile analysis of laser-welded aluminum alloy

Ir. Muchiar, S Yoshida, R. Widiastuti, A. Kusnovo, K. Takahashi, S. Sato

Application of slip-band visualization technique to tensile analysis of laser-welded aluminum alloy

Muchiar, S. Yoshida, R. Widiastuti, and A. Kusnowo
Research and Development Center for Applied Physics, Indonesian Institute of Sciences
P3FT-LIPI, PUSPIPTEK, Serpong, Indonesia 15320

K. Takahashi and S. Sato
Laser Laboratory, Institute of Research and Innovation
1201 Takada, Kashiwa, Chiba 277 Japan

ABSTRACT

Recently we have developed a new optical interferometric technique capable of visualizing slip band occurring in a deforming solid-state object. In this work we applied this technique to a tensile analysis of laser-welded aluminum plate samples, and successfully revealed stress concentration that shows strong relationships with the tensile strength and the fracture mechanism. We believe that this method is a new, convenient way to analyze the deformation characteristics of welded objects and evaluate the quality of welding.

The analysis has been made for several types of aluminum alloys under various welding conditions, and has shown the following general results. When the penetration is deep, a slip band starts appearing at the fusion zone in an early stage of the elastic region of the strain-stress curve and stays there till the sample fractures at that point. When the penetration is shallow, a slip band appears only after the yield point and moves vigorously over the whole surface of the sample till a late stage of plastic deformation when the slip band stays at the fusion zone where the sample eventually fractures. When the penetration depth is medium, some intermediate situation of the above two extreme cases is observed.

Keywords: speckle interferometry, white-band, slip-band, mesomechanics, mesoband, void

1. INTRODUCTION

Based on electronic speckle interferometry, we developed a new technique for visualize slip-band occurring in deforming solid stae object. In the new technique we use two pairs of dual-beam speckle pattern interferometer. This interferometers used for observing the deformation or deflection of the object in the vertical and horizontal directions respectively.

The slip-band or usually we call it the white-band (WB), because in our black and white monitor appears as brightest band, occurring as a result of subtraction of the speckle image before and after deformation. The WB become interesting because from our experiences, the WB or slip-band has a relation with a deformation on the plastic region and fracture. From the new theory of plastic deformation and fracture, developed by V.E. Panin et.al., the WB can be explained as a slip-band, which has an essential role in a late stages of plastic deformation and fracture.

In our experience with aluminum samples under tensile load, by knowing the number, shape and movement of the WB, we can estimate whether the object close to fracture and when the fracture will occur. If appear more than one WB and/or moving along the surface image of the object, we can predict that the possibility of the object become fracture is low. If the WB becomes stationary on the object surface image, we can predict that the object is close to fracture and fracture will occur on the position of the white-band.

From this experience we believe that we can use this visualization technique of white-band or slip-band for analyzing the characteristics of welding objects and evaluate the welding results.

2. THEORITICAL BASIS

V.E. Panin et.al., recently developed a new theory about plastic deformation and fracture of solid state on the basis of physical mesomechanics. The plastic deformation of a solid under loading is related to a loss of its shear stability and is being developed as a multilevel relaxation process[1]. There are three scale-levels in the plastic deformation growth, the level are micro, meso, and macro levels. In each level, stress concentrator generates defect and as a relaxation process the defects propagate in in the material and causing translational deformation. A mesoband is formed when mesoscale defects propagate, and cause vortices. In early stages of plastic deformation, the mesoband is formed at various location of the

object, in the direction of maximum shear-stress. In these stages, the stress concentration is still on a local level and the deformation represented by the mesobands is restricted in local area. When the deformation reaches the macro-level, translational-rotational vortex are integrated into a few vortices. Under this condition, the deformation is localized at the boundaries of these macro-scale vortices. In this stage, the stress concentration is still in a local level . When the deformation reaches the final stage, the stress concentration grows to the global level, and the meso band represents the deformation occurring in the object as a whole, and becomes stationary at a certain location.

The white-band is best explained as a mesoband on the macrolevel. The white-band have many common properties with mesoband, such as running in the direction of the maximum shear-stress, representing local deformation. The moving white-band represents mesobands occurring at various location at different time, the decrease of the WB number can be interpreted as the integration of the tranlational-rotational vortex, and the stationary Wb represents a mesoband appears at the final stage of deformation which lead to fracture.

3. EXPERIMENTAL

3.1. Experimental set-up and procedure.

Figure 1 illustrates the experimental set-up to observe the white-band. The optical set-up consist of two identical dual-beam electronic speckle pattern interferometer. One interferometer set in the vertical position and relatively sensitive for observing the displacement only in this direction. The other interferometer set in the horizontal position and also relatively sensitive in this horizontal direction. Furthermore, we call these interferometers as a vertical and a horizontal interferometer, respectively. In each interferometer we used a 25-mWatt He-Ne laser, as a light source, A universal-testing-machines (UTM) is used to test the object. In this experiment we use the tensile speed 0.35 mm/min. During the process, the speckle images of the object surface is taken by a CCD camera, then transfer to the frame memory and store in the computer memory for subtraction.

The recording process started with recording a speckle image of the object illuminated by the vertical interferometer alone. This recorded speckle image called $I_{b,v}$. As soon as $I_{b,v}$ was taken, we switched from a vertical interferometer to a horizontal interferometer and recorded the speckle image formed by the horizontal interferometer, this recorded speckle image called $I_{b,h}$. After that, we switched back to the vertical interferometer and after a deformation interval of Δt = 5 to 6 s, recorded speckle images $I_{a,v}$ and $I_{a,h}$, respectively, in the same way as $I_{b,v}$ and $I_{b,h}$. These $I_{a,v}$ and $I_{a,h}$ then subtracted from $I_{b,v}$ $I_{b,h}$, respectively, to form vertical fringe pattern (VFP) and horizontal fringe pattern (HFP). The switching times from the vertical to horizontal interferometers were set as fast as possible, so that the two patterns may effectively correspond to the same time. This procedure is repeated with data acquisition interval of ΔT = 10 to 14 s until the object fracture.

3.2 Specimens

As an object we used a specimen with effective length 150 mm, 25 mm wide, and 2 mm thick, and made of standard aluminum plate. There are five kind of specimens we used: (1) The non-welded (NW) specimens; (2) Shallow-welded (SW) specimens; (3) Deep-welded (DW) specimens; (4) Butt-joint welded (BW) specimens; (5) Graphite-coating welded (GW) specimens. The non-welded specimens are made of aluminum standard aluminum type A5052P-H112 and all welded specimens are made of standard alminum type A5052P-H32 and welded by CO_2 laser with shielding gas are Argon at flow rate 40 l/min. SW, DW, and BW specimens were welded with effective laser power 3,75 kWatt., and welding speed, respectively, 6.0 m/min., 2.0 m/min., and 2.0 m/min. Whereas, the GW specimens welded with effective power laser 3,0 kWatt and welding speed 2.5 m/min.

4. RESULTS AND DISCUSSION

4.1. Non-welded specimens.

The white-band or slip-band occurring after we subtracted the $I_{a,v}$ from $I_{b,v}$ and $I_{a,h}$ from $I_{b,h}$. In the interference pattern of the speckle image (VFP or HFP) the WB appears as the brightest band. on the black and white monitor crossing the usual interference fringes. Figure 2 shows the picture of the white-band in a few different locations of the non-welded specimen. This figure also shows the curve of the movement expressed by the WB location in the pixel number as a function of the serial data acquisition, and the curve of the stress-strain curve expressed by the tensile load in kN as a function of object elongation in mm. In this case, the first WB appears after the yield point (point A), move up and down vigorously along the speckle image on the plasticity region, and become stationary in the location of fracture. If the fracture time is relatively long, the direction and/or the number of WB may changes. But near the fracture time, the position and direction of the WB become stationary, and fracture occur in this location.

Depending on the plastic deformation stages, we can differentiate the characteristics of the WB, as follows:

- In the early stage of plastic deformation, more then one WB appears together. It move up and down vigorously along the image surface, and the direction may changes 180°.
- In the middle stage, the number of WB decrease until only one WB remain, but mnovement still happen.
- In the late stage of plastic deformation, the WB becomes stationary at the fracture location.

4.2. Welded-specimens.

Figure 3 shows the curve of the WB position as function of data number, the curve of stress-strain as function of elongation, and the picture of the cross-section of the bead, respectively, for shallow, deep, but-joint, and graphite coating welded specimens. From the stress-strain curve it can be seen that the first WB does not appear in the same elongation. For the SW specimens, the first WB appear after yield point, at the data number 75, and under tensile load 6.0 kN. The characteristic looks like the characteristic of the non-welded specimen, but the frequency of movement is lower. For the DW, BW, and GW specimens, the first WB appear at the tensile load 4.0, 3.5, and 0.3 kN, respectively. In the stress-strain curve, the position is on the elastic region. A little movement only happen in the DW specimen, but for the BW and GW specimen, the WB characteristics are completely different, the WB still stationary until the fracture in the location where it is first appear. From the cross-section of the bead it can be observed that the void in the bead does not similar. No void in the SW specimens, a little number of voids in DW specimens, and a large number of voids in the GW specimens.

According to mesomechanics, the WB is identical with meso or macro-band. So, the WB only shows the local effect , not a global effect or integrated effect as yield load or ultimate load in the stress-strain curve . Therefore, in the case of DW and especially for BW and GW specimens, the voids formed in the fusion zone will cause a pre-strain in the specimens. The pre-strain becomes larger if the number of the voids becomes larger and smaller if the numbers is smaller. Under a tensile load the relaxation process will grow from this location. If the pre-strain is larger, the tensile load relaxed intensively at this location before the other parts reach the level in which they can show a white-band. So far, we always see the WB stationary in same position until the fracture, and this is the case of the BW and GW specimens. If the pre-strain is small, in the case of the DW specimens, there is enough time for the other parts reach the level in which the WB to appear, but the voids causes the first white-band appear in the elastic region of the global effect, and the frequency of movement is low. For the SW specimens, because there is no void in the bead, the WB characteristic looks like the non-welded specimen characteristics.

Because the white-band only shows the local effect, we cannot predict the yield load or the ultimate load. But the white-band has a relationship with timing and location of fracture, and the first type of white band can guess a void density.

5. CONCLUSIONS

From the results of the experiment, we can conclude two indicators for tensile strength of welded joint. First, the appearances of the first white-band maybe after or before yield point and the location maybe in the plastic region or elastic region. In the case of with-band appear after yield-point or in the plastic region, it will move up and down vigorously and become stationary in the location of fracture. In the case of white-band appear in the elastic region, it always stays in one location until fracture. Second, there are a relationship between the appearance of the white-band and a void density.

6. REFERENCES

1. S. Yoshida, Suprapedi, R. Widiastuti, Marincan, Septriyanti, Julinda, Faizal, and A.Kusnowo, submitted JJAP Letters.
2. V.E. Panin, "Physical mesomechanics of plastic deformation and experimental results obtained by optical methods", Oyo Buturi, vol.64 (1995), No.9, 888.
3. S. Yoshida, Suprapedi, R. Widiastuti, Marincan, Septriyanti, Julinda, Faizal, and A.Kusnowo, "A novel, optical nondestructive deformation analyzer based on electronic speckle pattern interferometry and a new plastic deformation theory", Abstract Proceedings of the VIII International Congress on Experimental Mechanics and Experimental/ Numerical Mechanics in Electronic Packaging, 168, Nashville,USA, June 1996

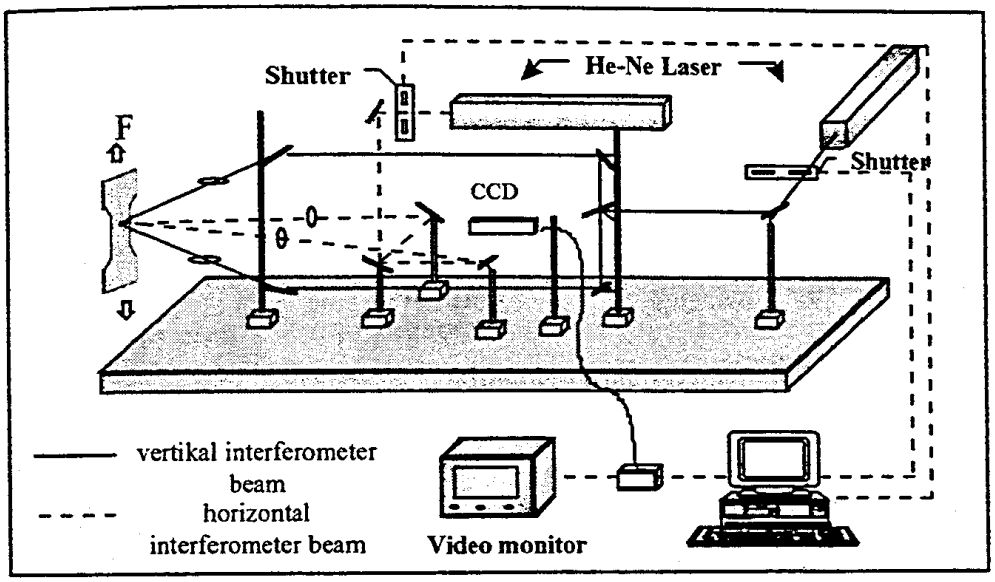

Figure 1. Experimental set-up

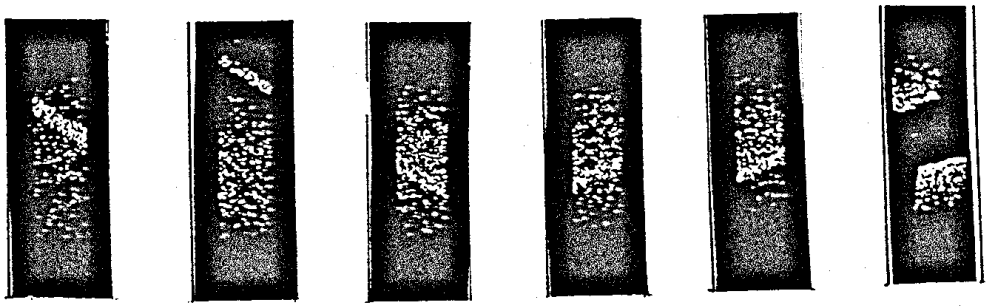

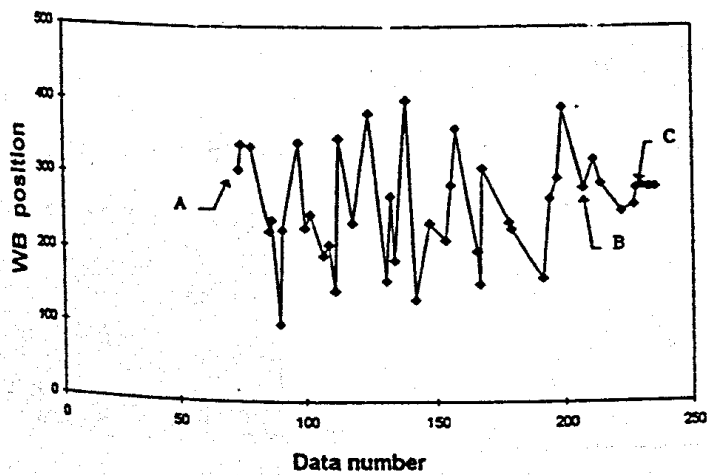

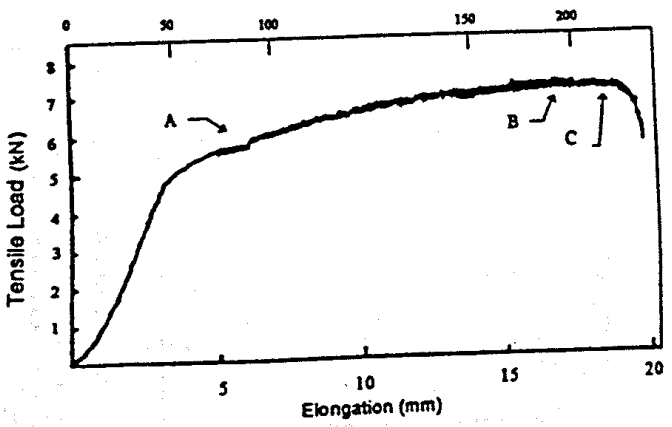

Figure 2. The characteristics of non-welded specimens

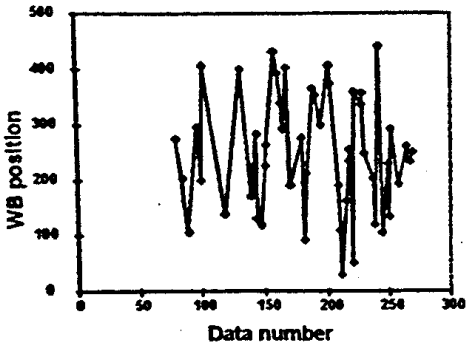

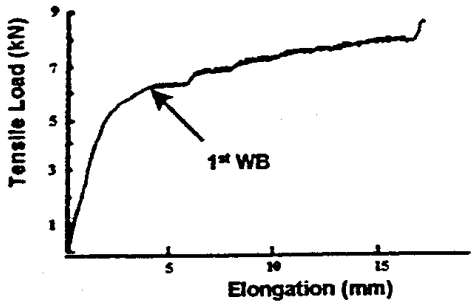

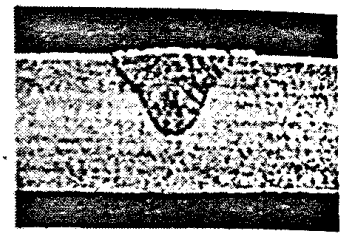

A. Shallow-welded

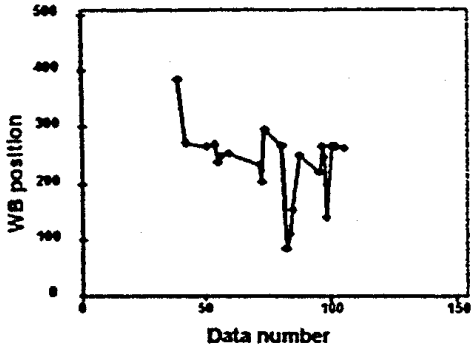

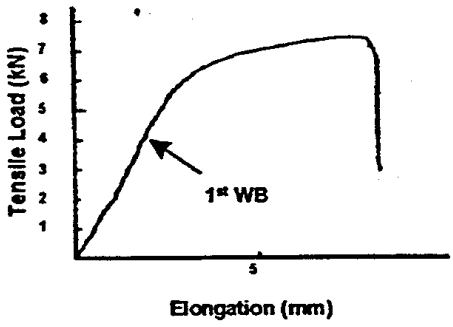

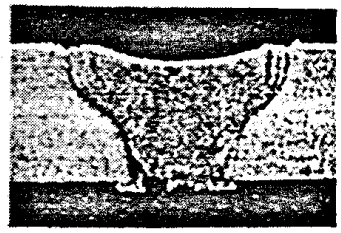

B. Deep-welded

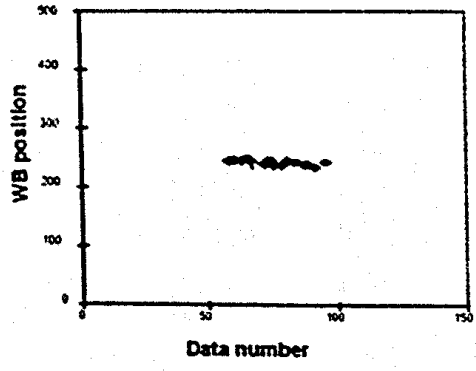

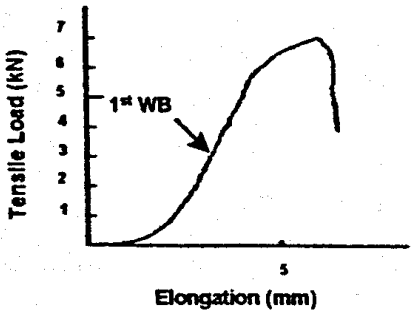

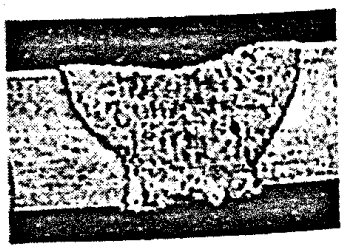

C. Butt-joint welded

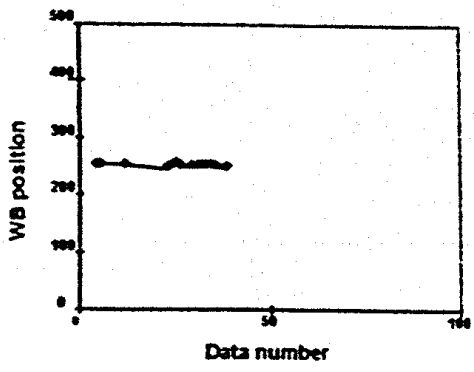

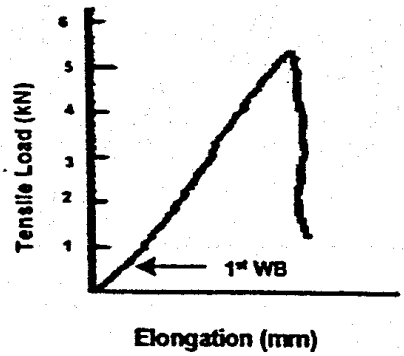

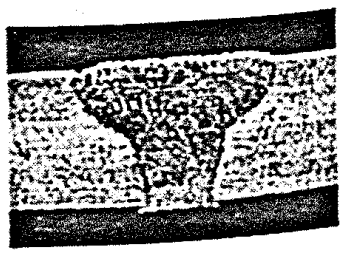

D. Graphite-coating welded

Figure 3. Characteristic of laser-welded specimens